Catena 220 (2023) 106634

Contents lists available at ScienceDirect

Catena

journal homepage: www.elsevier.com/locate/catena

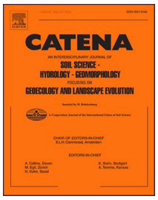

Influence of degree of compaction on arsenic and antimony co-contaminated soil stabilization: Geoenvironmental properties and chemical species

Shi-Ji Zhou [a], Ya-Song Feng [b], Guang-Yu Yang [a], Hui-Yang Sun [a], Qing Zhang [a], Yang Hu [a], Yan-Jun Du [a,*]

[a] *Jiangsu Key Laboratory of Urban Underground Engineering & Environmental Safety, Institute of Geotechnical Engineering, Southeast University, Nanjing 211189, China*

[b] *Jiangsu Province Key Laboratory of Environmental Engineering, Jiangsu Provincial Academy of Environmental Science, Nanjing 210036, China*

ARTICLE INFO

Keywords:
As and Sb contaminated soil
Stabilization
Degree of compaction
Semi-dynamic leaching test
CT and XPS analyses

ABSTRACT

The current research and engineering practice lack adequate consideration of the influence of degree of compaction (DOC) on the stabilization efficiency and the long-term performance of stabilized contaminated soil. This study investigated the influence of DOC on the characteristics of an iron-based stabilizer amended As and Sb contaminated soil. The stabilizer was labelled as PFSC and was a mixture of polymerized ferric sulfate (PFS) and hydrated lime with a dry mass ratio of 2:1. Various tests were conducted to determine the metalloids leachability (HJ 557), unconfined compressive strength (UCS) (ASTM D1633), and hydraulic conductivity (k_w) (ASTM D5084) of stabilized contaminated soil with different DOC (ranged from 75% to 96%). A semi-dynamic leaching test following US EPA Method 1315 was performed on soil specimens to explore the leaching controlling mechanisms and determine the observed diffusion coefficients (D^{obs}) of metalloids releases when diffusion was the controlling mechanism. The influence of DOC on soil pore characteristics and elements' valence states were investigated by X-ray computed tomography (CT) and X-ray photoelectron spectroscope (XPS). As the DOC increased, the UCS of soil specimens increased from 4.26 to 43.78 kPa, while the k_w decreased form 1.33×10^{-7} to 2.81×10^{-9} m s^{-1}. DOC shows different influences on As and Sb leached concentrations. The mean D^{obs} for As and Sb released form soil specimen with DOC of 96% were 3 and 2 orders of magnitude lower than that of 75%. CT analysis results indicated the macropore number and macropore size in soil specimens were reduced with the increasing DOC. XPS analysis results suggested compaction promoted the specie transformation of As, Sb, and Fe from As(V) to As(III), from Sb(V) to Sb(III), and Fe(III) to Fe(II)., respectively. The pore filling and chemical specie transformation jointly determined the releases of metalloids from stabilized contaminated soil specimen.

1. Introduction

Arsenic (As) and antimony (Sb) are metalloid elements considered to behave similarly and display the same range of oxidation states (−3 to +5) in the soil environment (Johnston et al., 2020; Wilson et al., 2010). The toxicities and mobilities of metalloids are dependent on their species and the chemical phase of the coexisting compounds (Filella et al., 2002). Both metalloids most commonly occur in the +5 state in oxic environments (arsenates (As(V)) and antimonates (Sb(V))) and in the +3 state in anoxic environments (arsenites (As(III)) and antimonites (Sb (III))) (Wilson et al., 2010). The general order of toxicity and mobility for As and Sb species are given as: Organoarsenicals < As(V) < As(III) and organoantimonials < Sb(V) < Sb(III), respectively (Wilson et al., 2010). System pH and oxidation–reduction potential (Eh) largely determine As and Sb oxidation states and environmental reactions in soil (Wilson et al., 2010). The metalloid properties of As and Sb ensure them strong affinity on clay minerals, iron oxygen, and hydroxide. Various types of surface binding site have reported for As(V) and As(III) affinity on iron surfaces, including monodentate complexes, bidentate binuclear complexes, and mononuclear complexes (Ona-Nguema et al., 2005).

---

* Corresponding author.
E-mail addresses: shijizhou@seu.edu.cn (S.-J. Zhou), fengyasong@seu.edu.cn (Y.-S. Feng), 220193259@seu.edu.cn (G.-Y. Yang), 220193200@seu.edu.cn (H.-Y. Sun), 220203222@seu.edu.cn (Q. Zhang), seuhy@seu.edu.cn (Y. Hu), duyanjun@seu.edu.cn (Y.-J. Du).

https://doi.org/10.1016/j.catena.2022.106634
Received 31 July 2022; Received in revised form 7 September 2022; Accepted 10 September 2022

Similar to As, Sb on Fe oxides and hydroxides surfaces form bidentate and corner-sharing inner-sphere complexes (Leuz et al., 2006). Furthermore, the affinity of As and Sb on Fe oxides and hydroxides is important for their retention in soils (Fritzsche et al., 2006; Krysiak and Karczewska, 2007).

Soil contaminated with As and Sb would impose risks to human health and be hazardous to the ecological environment (Ko et al., 2012; Liu et al., 2010; Zhang et al., 2009). The majority of As and Sb contaminations appear to originate from mining and smelting operations and co-occur frequently nearby the mining sites (Fawcett et al., 2015; Johnston et al., 2020; Telford et al., 2009). Remediation of metalloids contaminated soil can be achieved by various techniques, such as phytoremediation (Madejón et al., 2018; Shetty et al., 2021), electrokinetic remediation, and biological treatment (Ko et al., 2017; Li et al., 2020; Yuan and Chiang, 2008), solidification/stabilization (S/S) (Álvarez-Ayuso et al., 2013; Bagherifam et al., 2014; Feng et al., 2021; Ko et al., 2012; Xia et al., 2019b, 2019a; Zhang et al., 2020). Stabilization is one of the most cost-effective techniques and widely applied in metalloids contaminated soil remediation and risk management in China (An et al., 2019; Xu et al., 2021; Zhao et al., 2017). Recently, a new iron-based stabilizer was developed to stabilize soil co-contaminated with As and Sb (Zhou et al., 2022a). This stabilizer, term as PFSC, is a mixture of polymeric ferric sulfate (PFS) and hydrated lime ($Ca(OH)_2$) in a proportion of 2:1 by dry weight basis, as the ratio yielded a relatively low leached concentrations of As and Sb (Zhou et al., 2022a). It is suggested that PFSC can effectively immobilize As and Sb by transforming leachable As and Sb fractions into Fe-Mn oxides bound fractions (Zhou et al., 2022a).

There are two major methods of applying stabilization to contaminated soil: *ex-situ* stabilization (Feng et al., 2020; Vrînceanu et al., 2019; Xia et al., 2019a) and *in-situ* stabilization (Xia et al., 2019b). The *ex-situ* stabilization entails excavating contaminated soil and transporting it to a different location, either *on-site* or *off-site*, for subsequent mixing with reagents (Feng et al., 2020; Xia et al., 2019a). *In-situ* stabilization involves mixing reagents into the contaminated soil in the place where it is existed and thus does not involve excavation and transport to another location (Xia et al., 2019b). There are many factors that influence the efficiency of stabilization, including stabilizer dosage, moisture content of the contaminated soil, curing time for stabilized contaminated soil, and the mixing efficiency of the stabilizer with contaminated soil (Feng et al., 2021; Wang et al., 2015a, 2015b; Xia et al., 2019b, 2019a; Zhou et al., 2022a). Compaction is a necessary step during the *ex-situ* stabilization processes when the stabilized contaminated soil is backfilled in site and disposed in a landfill (Feng et al., 2022; Xue et al., 2014; Zhou et al., 2022a)., The compactness of contaminated soil increased with depth due to an increase of overburden pressure for *in-situ* stabilization. Xue et al., (2014) investigated the effect of degree of compaction (DOC) on the properties of cement-solidified lead contaminated soil, finding that the DOC determined the properties by influencing the formation of hydration products as well as the microscopic morphology and pore distribution of the solidified bodies. Compared to Pb, As and Sb have various species and more complex geochemical behavior in the soli environment (Nakamaru et al., 2006; Quiroz et al., 2016; Wilson et al., 2010). However, the current research and engineering practice lack adequate consideration of the influence of DOC on the stabilization efficiency and the long-term performance of stabilized contaminated soil.

The purpose of this study was to investigate the influence of DOC on geoenvironmental properties of PFSC stabilized As and Sb contaminated soil. The metalloids leached concentrations, unconfined compressive strength (UCS), and hydraulic conductivity (k_w) of soil specimens compacted with different degrees were determined. The leachability of contaminants is the indicative parameter used to evaluate the environmental safety of stabilized contaminated soil. The unconfined compressive strength presents the performance of stabilized contaminated soils when they reused as civil engineering materials, such as embankment filling, which has bearing capacity requirements according to the application scenarios. The k_w of stabilized contaminated soils effects their long-term safety and the migration of contaminants to the surrounding soil and groundwater. Furthermore, A semi-dynamic leaching test was conducted to evaluate the influence of DOC on the long-term leaching characteristics of soil specimens, including cumulative leached fraction, controlling mechanism, and observed diffusion coefficient (D^{obs}). The influence of DOC on micromorphology of PFSC stabilized contaminated soil was analyzed, and the reduction processes of As, Sb, and Fe in the soil samples with increasing DOC were also measured.

2. Materials and methods

2.1. Contaminated soil and PFSC stabilizer

Arsenic and Sb contaminated soil used in this study had a silty clay (SC) texture and was collected from an abandoned arsenic factory site (longitude: $107^\circ 59' 51.00''$, latitude: $24^\circ 32' 31.43''$). The physicochemical properties and oxide compositions of the contaminated soil were presented in Zhou et al., (2022a) and provided in Table S1 and Table S2. The total metalloids concentrations (6547 ± 362 and 2420 ± 217 mg kg^{-1} for As and Sb, respectively) of the contaminated soil were exceed the risk intervention values of category II developed land regulated in China GB 36600. Before being used in this study, the contaminated soil was air-dried, crushed, ground to pass through a 2 mm nylon sieve, and stored in room conditions. Before the laboratory experiment, the PFSC was prepared by PFS and hydrated lime in a 2:1 ratio by weight using an auto-electric mixer for 15 min to obtain visual homogeneity. The PFSC consists of 53.5% CaO, 27.6% Fe_2O_3, 14.4% SO_3, 1.3% MgO, and 0.9% SiO_2, measured using a X-ray fluorescence spectrometry (XRF, Thermo Fisher Scientific, ARL9800XP+).

2.2. Soil specimen preparation

The detailed information on cylindrical soil specimens used for the unconfined compression strength (UCS) test, batch leaching test, flexible-wall hydraulic conductivity (k_w) test, and semi-dynamic leaching test were presented in Table S3. All the soil specimens were prepared at the PFSC dosage of 4% and the moisture content of 21%. With 4% PFSC, the As and Sb leached concentrations were 0.25 and 0.13 mg L^{-1}, respectively, which were closed to the remediation targets of the studied contaminated soil (0.5 and 0.05 mg L^{-1} for As and Sb, respectively) (Zhou et al., 2022b). The degree of compaction (DOC) of soil specimens were set to 75%, 80%, 85%, 90%, 93%, and 96%, which were given as:

$$K = \frac{\rho}{\rho_{dmax}} \times 100\% \tag{1}$$

where K is the DOC of soil specimen (%), ρ_{dmax} is the maximum dry density of the untreated contaminated soil (1.68 g cm^{-3} in this study), and ρ is the dry density of soil specimen used for the various tests (g cm^{-3}). The influence of adding PFSC on ρ_{dmax} of contaminated soil was unconsidered due to the low dosage of 4%. Cylindrical molds with the given diameters and heights (Table S3) were used to produce the samples. Fig. S1 presents the examples for compacted granular soil holder, compacted soil specimen, and 1-D semi-dynamic leaching setup. The predetermined amount of contaminated soil, PFSC, and deionized water were mixed, transferred into the cylindrical mold, and statically compacted to obtain the desired density. Then, the cylindrical soil specimen was extruded from the mold, sealed in a resealable bag, and cured for 14 d under a curing condition with a temperature of 20 ± 2℃ and humidity of 95%.

2.3. UCS, k_w, and leaching test

The UCS and k_w tests conducted to soil specimens compacted with different degrees were carried out as per ASTM D1633 and ASTM

D5084, respectively. An automatic loading apparatus with a maximum capacity of 10 kN and a flexible-wall system were used. During the UCS test, the load was applied to the soil specimen at a displacement rate of 1.0 mm min^{-1} and the maximum load was recorded. The k_w testing procedures, including flexible rubber membrane encompassment, filter paper and porous stone equipment, soil specimen saturation, and permeation, were same to that described by Zhou et al., (2022a). The k_w test was conducted under the effective confining stress of 75 kPa and the seepage stress of 50 kPa. Tap water was used as the permeant solution, and the pH value and EC value of the tap water was measured to 7.16 and 143 μs cm^{-1}, respectively. Each soil specimen was permeated until the termination criteria were achieved, and the final hydraulic conductivity (k_f) was calculated as the mean value of the final four measurements.

A deionized water leaching test was conducted to determine the leached characteristics of stabilized contaminated soil samples compacted with different degrees. The soil sample (100 g, dry mass) with soil particle size less than 30 mm and 1000 ml deionized water were mixed in a 2000 ml polyethylene bottle, and shaken at the rate of 110 ± 10 rpm for 8 h in a horizontal vibration apparatus. The metalloids concentrations in the leached liquid were measured using an ICP-OES instrument after performing the filtration using a 0.45 μm GHP filter. The soil pH was determined at an S/L ratio of 1:1 as per Method 9045D. The soil Eh was also determined as per HJ 746 under the protection of purity nitrogen.

2.4. Method 1315 semi-dynamic leaching test

The Method 1315 semi-dynamic leaching test was conducted to stabilize contaminated soil specimens compacted with different degrees to evaluate metalloids releases, and the distilled water was used as a leaching agent. After the designed curing age, the soil specimens were rinsed by immersion in distilled water and then immediately placed within the weighed test vessel. The leachant was added to the vessel directly after the specimen was placed, and the volume of the leachant was determined according to the liquid volume-the sample geometric surface area (19.63 cm^2 in this study) ratio of 10. The test interval timing starts once the specimen was completely immersed in the leachant. The sample was not agitated during the leaching interval, and the temperature during the leaching test was maintained between 17.5 and 27.5 ℃. As specified by the Method 1315, the leachate was collected and entirely replaced at designated leaching intervals (0.08, 1.0, 2.0, 7.0, 14.0, 28.0, 42.0, 49.0, and 63.0 d). At the end of each test interval, the leachate was extracted by a 20 ml plastic syringe and filtrated by a 0.45 μm pore size membrane filter for As and Sb concentrations analysis. The specimen was removed from the vessel and placed into another leaching test vessel that already contains the appropriate volume of fresh leachant. The mass of the newly added leachant was calculated by subtracting the quality of the vessel, seal, and specimen from the mass of the assembled vessel. Repeat the test interval processes until the number of desired intervals has been performed.

The concentrations of As and Sb were analyzed, and the cumulative fraction leached (CFL) of metalloids was calculated using Eq. (2) (Li et al., 2017a), and its plot against leaching time square root ($t^{1/2}$) enabled the calculation of D^{obs} using Eq. (3). If diffusion is the dominant mechanism, t relationship between cumulative release and D^{obs} can be described as Eq. (4).

$$\mathrm{CFL} = \frac{A_t}{A_0} = \frac{1}{A_0}\sum_i (c_i \times V_i) \tag{2}$$

$$D^{obs} = \frac{\pi}{4} \times \left(\frac{V}{S}\right)^2 \times \frac{\mathrm{CFL}^2}{t} \tag{3}$$

$$\log(B_t) = \frac{1}{2}\log(t) + \log\left(U_{max} d \sqrt{\frac{D^{obs}}{\pi}}\right) \tag{4}$$

where A_t is the cumulative quality of the concerned substance released from the specimen (mg); A_0 is the amount of contaminant contained in the specimen before conducted to leaching test (mg); c_i is leached concentration contaminant at the leaching interval of i (mg L^{-1}); V_i is the volume of the leachate (L, 196.3 × 10^{-3} L in this study); V is the specimen volume (cm^3, 117.75 cm^3 in this study); S is the geometric surface of the specimen (cm^2, 19.63 cm^2 in this study); t is the contact time in second; $Umax$ is the maximum leachable mass (mg kg^{-1}); d is the bulk density of the specimen (kg m^{-3}).

2.5. CT and XPS measurements

The microscopic pore structure characteristics of stabilized contaminated soil specimens compacted with different degrees were investigated by Phoenix Vtomex S high-resolution X-ray CT instrument. This instrument uses a 240 kV X-ray source and a pair of linear array detectors to image soil specimens at constant-angle intervals through a full rotation (Ketcham, 2005; Wang et al., 2014, 2014), and the resulting data were used to reconstruct a sample cross-section.

The surface compositions and the chemical oxidation states of As, Sb, and Fe in stabilized contaminated soil samples compacted with different degrees (75%, 90%, and 96%) were determined using an ESCA and AES system (Surface Nano Analysis, GmbH, Germany) XPS instrument, which equipped with Al-kα (1486.6 eV) X-ray source (Huang et al., 2014). During the XPS measurement, the soil sample was placed on a double-sided carbon tape and a pass energy of 50 eV was used. Before the peaks were deconvoluted and quantified using the CASA software, the binding energies were calibrated by the C 1 s peak of 284.6 eV (Huang et al., 2014). The As 2p, Sb 3d, and Fe 2p peaks were taken as GL (30) [Gaussian to Lorentzian with Gaussian: 30%] and the percentage area coverage in each peak corresponding to a specific chemical oxidation state was calculated (Ajith et al., 2019).

3. Results and analyses

3.1. UCS and k_w

The UCS of soil specimens with various degrees of compaction (DOC) are presented in Fig. 1(a). Zhou et al., (2022a) suggested that PFSC stabilization increased the UCS of contaminated soil through pore filling provided by reaction products, such as iron oxide, iron hydroxide, and calcium sulfate. Fig. 1(a) shows that the UCS of PFSC soil specimens increased with increasing DOC. The UCS of PFSC stabilized contaminated soil specimens were 4.26, 7.43, 12.82, 28.33, 35.16, and 43.78 kPa with the DOC of 75%, 80%, 85%, 90%, 93%, and 96%, respectively. The UCS of PFSC stabilized contaminated soil specimen improved by increasing the DOC because of the reduction of pore volume (van Verseveld and Gebert, 2020; Xue et al., 2014). Furthermore, Xue et al., (2014) suggested that the strength of the cement solidified soil was associated with the hydration products, and the DOC influence the reaction products of the cement-Pb contaminated soil system. The DOC could affect the chemical reaction products of PFSC by influencing the availability of oxygen (O_2) (van Verseveld and Gebert, 2020). However, the influence of DOC on the chemical reaction products of PFSC stabilized contaminated soil as well as the UCS of the soil specimen need further investigation.

The long-term environmental safety property of the stabilized contaminated soil should be concerned in its further disposal process (Feng et al., 2021). The k_w indicates the migration of leachate substance through the stabilized contaminated soil into ambient soil and groundwater (Zhou et al., 2022a). Fig. 1(b) shows the k_w of soil specimens compacted with different degrees. The k_w of soil specimen with a DOC of

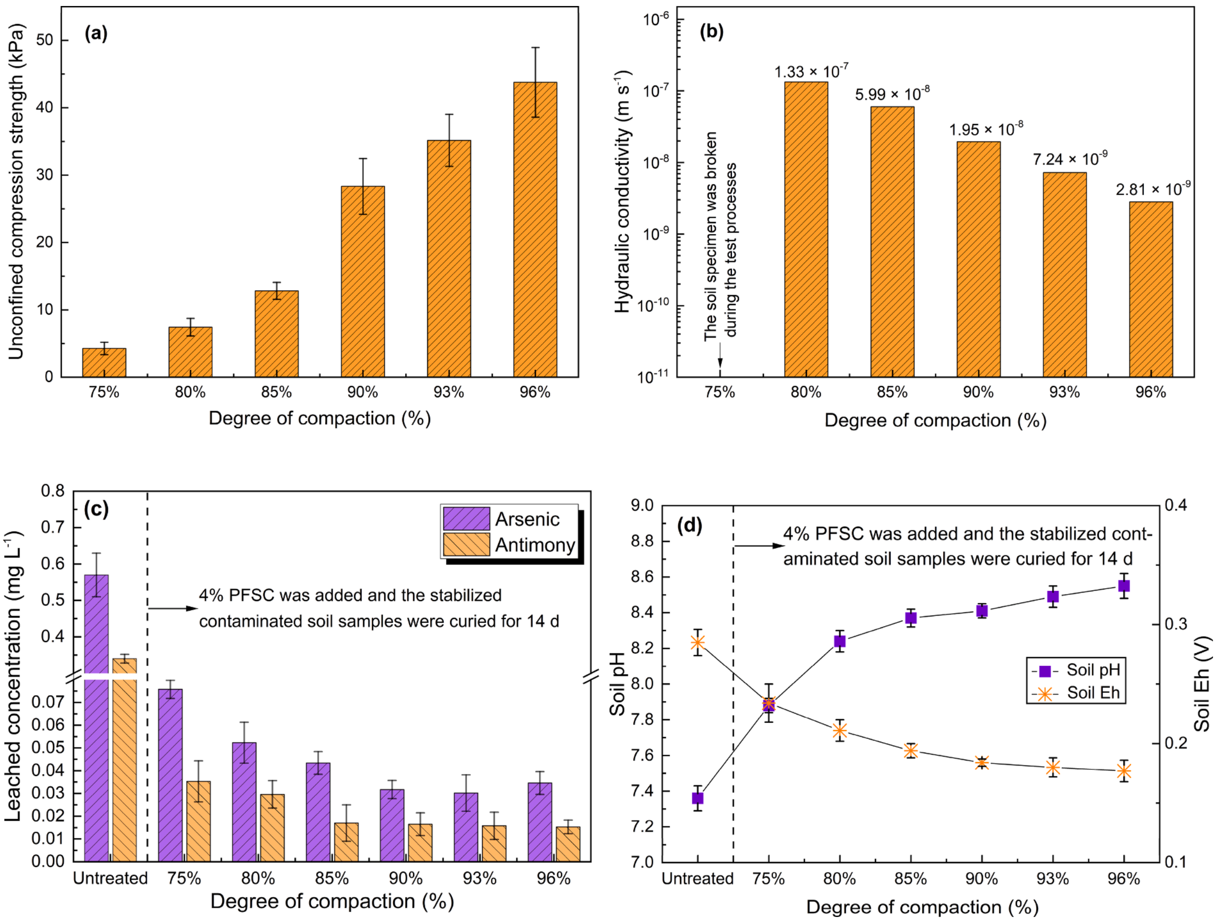

Fig. 1. The (a) unconfined compression strength (UCS) values, (b) hydraulic conductivities (k_w), (c) As and Sb leached concentrations and (d) soil pH and soil Eh values of PFSC stabilized contaminated soil specimens compacted with different degrees.

75% was unavailable because the specimen was broken during the flexible rubber membrane encompassment process due to its unconsolidated characteristic. As shown in Fig. 1(b), the k_w values of soil specimens were 1.33 × 10^{-7}, 5.99 × 10^{-8}, 1.95 × 10^{-8}, 7.24 × 10^{-9}, and 2.81 × 10^{-9} m s^{-1} with the DOC of 80%, 85%, 90%, 93%, and 96%, respectively. The k_w of soil specimen decreased with increasing DOC. The k_w of soil specimen with DOC of 96% was two orders lower that of 80%. These results indicated DOC was a non-negligible factor that affected the permeability of PFSC stabilized contaminated soil. The high DOC reduced the k_w of the soil specimens by reducing their porosities (Xue et al., 2014). To ensure the long-term environmental safety of the amended contaminated soil, the maximum k_w of 1.0 × 10^{-8} m s^{-1} was recommended by USEPA. At this point, the DOC of the contaminated soil stabilized by PFSC should not be lower than 93%. Therefore, high DOC should obtain through heavy rollers when the PFSC stabilized contaminated soil was backfilled *in-site* and landfilled *off-site*. Moreover, the addition of cementitious materials would decrease the k_w of PFSC stabilized contaminated soil.

3.2. *Metalloid leaching concentration*

As the most important index to evaluate the stabilization efficiency for contaminated soil, the metalloids leached concentrations of soil samples compacted with different degrees conducted by the deionized water leaching test are presented in Fig. 1(c). The As and Sb leached concentrations of untreated contaminated soil were 0.57 and 0.34 mg L^{-1}, which exceed the Chinese criterion for groundwater quality of Class IV (0.05 and 0.01 mg L^{-1} for As and Sb, respectively) prescribed in GB/T 14848. After stabilization, the metalloids leached concentrations of soil were much lower than that of untreated contaminated soil and ranged from 0.03 to 0.076 and from 0.015 to 0.035 mg L^{-1}, indicating the stabilizer PFSC was efficient in immobilization metalloids (Zhou et al., 2022a). The As leached concentrations decreased with the DOC increased from 75% to 90% and then increased slightly afterward, whereas the Sb leached concentrations decreased with increased DOC. These results showed the DOC of around 90% allowed the suitable stabilization of metalloids contaminated soil using PFSC. The pH and oxidation–reduction potential (Eh) values of the leached solution were measured and the results are presented in Fig. 1(d). The leachate pH and Eh values of untreated contaminated soil were 7.36 and 285 mV, respectively. The addition of PFSC increased the leachate pH and decreased the leachate Eh values of contaminated soils, and the leachate pH and Eh values of PFSC stabilized contaminated soils compacted with different degrees ranged from 7.88 to 8.55 and 234 to 57 mV, respectively. The pH values increased while the Eh decreased with increasing DOC. Soil pH and Eh largely determine metalloid oxidation states and then influence the leachabilities of As and Sb (Fawcett et al., 2015; Smith et al., 1999; Wilson et al., 2010). As(V) and Sb(V) are less mobile than As(III) and Sb(III), respectively (Wilson et al., 2010). As(V) has an environmental solubility minimum around pH 4–6, and As(III) affinity on clay minerals increases with increasing pH between 3 and 9 (Frost and Griffin, 1977). The affinity of Sb(V) to clay minerals appears to be strong but more dependent on pH than that of Sb(III) with maximum adsorption below pH 7 (Leuz et al., 2006). The increased affinity of As and Sb on soil minerals and Fe oxides and oxyhydroxides result in the decreasing of metalloids leached concentrations. The reductive influence of elements on As and Sb speciation and mobility is considered later. The DOC of the PFSC stabilized contaminated soil can affect the pore structure characteristics and the chemical species of As, Sb, and Fe, which have been verified by the micromorphology tests.

3.3. Semi-dynamic leaching behavior

3.3.1. Cumulative fractions

The variations of metalloids leached concentrations with the leaching time for soil specimens compacted with different degrees under semi-dynamic leaching condition are shown in Fig. S2. The leached As and Sb increased more sharply during the initial 2 d and then decreased slightly. The soluble As and Sb would be dissolved in the initial leaching stage and resulted in highly leached concentrations. The leached metalloids concentrations decreased with the increasing of DOC, indicating the high risks to groundwater of soils in low DOC and low risks in high DOC. Therefore, an interlocking framework of PFSC stabilized contaminated soil could reduce the releases of As and Sb due to the pore filling in the matrix (Xue et al., 2014). The cumulative fractions of metalloids leached from soil specimens compacted with different degrees are plotted as a function of leaching time using a semi-log graph in Fig. 2(a) and Fig. 2(b), and the slopes and R2 values are summarized in Table 1. The cumulative fractions of As and Sb decreased with increased DOC of stabilized contaminated soil specimen. These results presented in Table S4 suggested that very low percentages of total metalloids were released from stabilized contaminated soil during the semi-dynamic leaching test. The cumulative fractions of As and Sb decreased with increasing DOC of PFSC stabilized contaminated soil specimens between 75% and 96%.

3.3.2. Leaching controlling mechanisms

The mechanisms controlling the releases of metalloids from soil specimens compacted with different degrees were investigated using the de Groot and van der Sloot diffusion model. The cumulative releases of As and Sb from soil specimens compacted with different degrees are plotted as a function of leaching time in Fig. 2(c) and Fig. 2(d). The slopes of each leaching interval for As and Sb release from stabilized contaminated soil specimens and the controlled mechanisms are presented in Table S5–S10. Wash-off, dissolution, and diffusion were the potentially mechanisms controlling As and Sb releases, which can be characterized by assessing the slope in Eq. (3). Furthermore, the slope value close to 0, 0.5, and 1 suggests that the release of the concerned substance was controlled by wash-off, dissolution, and diffusion, respectively. As and Sb releases from PFSC stabilized contaminated soil specimens were controlled by a mixed process of dissolution, diffusion,

Table 1
Regression analysis of As and Sb leaching parameters and observed diffusion coefficients (D^{obs}) for PFSC stabilized contaminated soil specimens compacted with different degrees.

Degree of compaction	Arsenic (As)			Antimony (Sb)		
	Slope	R^2	Mean D^{obs} ($cm^2\ s^{-1}$)	Slope	R^2	Mean D^{obs} ($cm^2\ s^{-1}$)
75%	0.43	0.86	1.92×10^{-8}	0.47	0.94	2.63×10^{-9}
80%	0.34	0.86	4.72×10^{-9}	0.46	0.93	1.93×10^{-9}
85%	0.35	0.87	1.41×10^{-9}	0.47	0.94	2.99×10^{-9}
90%	0.45	0.92	2.27×10^{-10}	0.44	0.94	2.04×10^{-10}
93%	0.45	0.93	1.28×10^{-10}	0.37	0.94	1.84×10^{-10}
96%	0.41	0.92	4.65×10^{-11}	0.38	0.93	4.10×10^{-11}

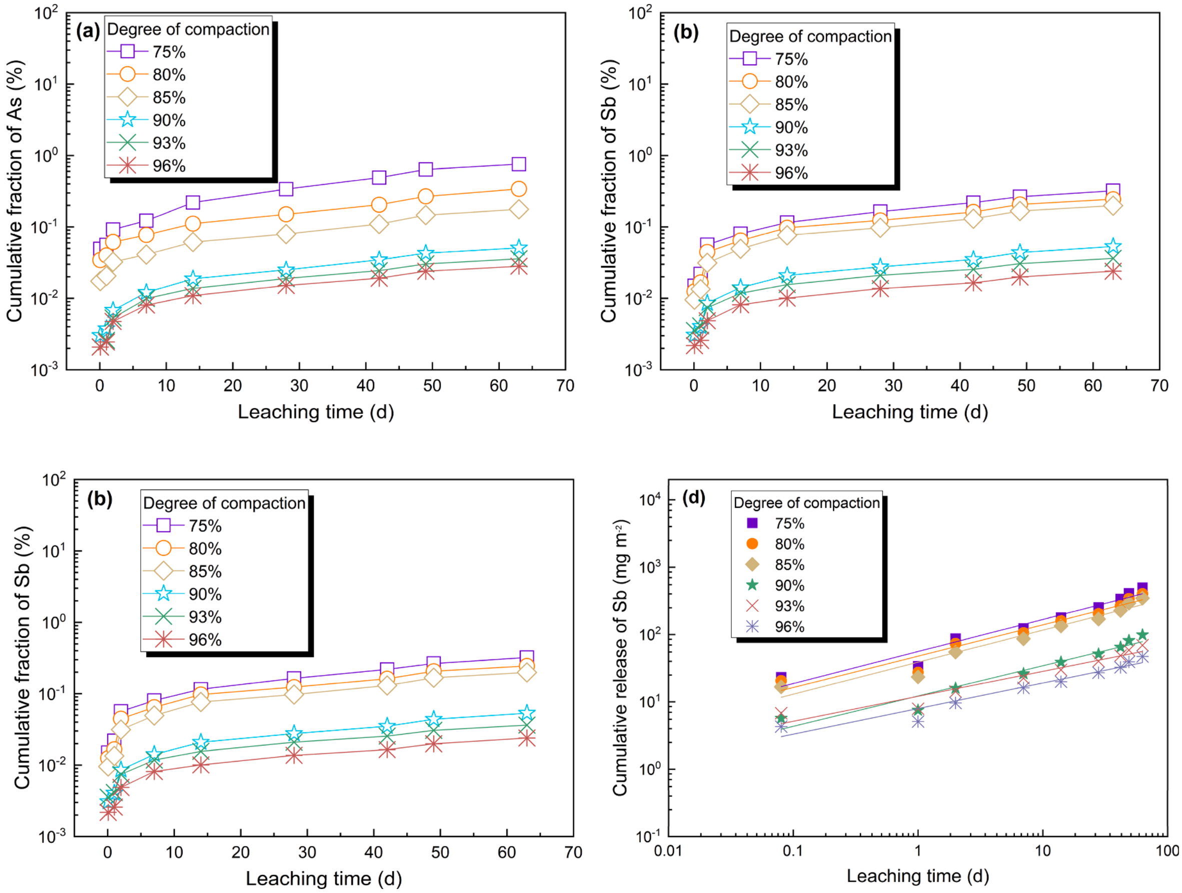

Fig. 2. The cumulative fractions of (a) As and (b) Sb and the cumulative releases of (c) As and (d) Sb released from PFSC stabilized contaminated soil specimens compacted with different degrees as a function of leaching time.

and wash-off, and diffusion appeared to be the main controlling mechanism with the increasing of DOC. As shown in Fig. S3, the specimens of PFSC stabilized contaminated soil with the DOC of 75%, 80%, and 85% were broken caused by hydraulic erosion and the contaminants were released into the solution during the leaching processes. Unlike the soil specimens with low DOC (75% and 80%), the DOC higher than 90% appeared to maintain the integration of soil specimens after the leaching test.

The influence of DOC on the leaching behavior of As and Sb for soil specimens was assessed based on the mean D^{obs}, which are presented in Table 1. The mean D^{obs} of PFSC stabilized contaminated soil specimens for As and Sb releases were ranged from 1.92×10^{-8} to 4.65×10^{-11} and from 2.63×10^{-8} to 4.10×10^{-11} $\mathrm{cm}^2\ \mathrm{s}^{-1}$ with the increasing DOC between 75% and 96%, respectively. The mean D^{obs} decreased with the increasing of DOC. The mean D^{obs} of PFSC stabilized contaminated soil specimens with a DOC of 96% for As and Sb releases were 3 and 2 orders of magnitude lower than that of 75%. Diffusivities are governed by geometrical pore characteristics of soils such as pore size distribution, tortuosity, porosity, and connectivity (Martínez et al., 2016; van Verseveld and Gebert, 2020). Compaction affects the releases of As and Sb by changing the microscopic pore characteristics of PFSC stabilized contaminated soil specimens.

3.4. CT analysis

CT analysis results of PFSC stabilized contaminated soil specimens compacted with different degrees are presented in Fig. 3, which suggested that the macropore number and macropore size in soil specimens were reduced with the increasing DOC. Grey images of soil specimens compacted with different degrees are presented in Fig. S4, the macropores are shown in black color, and the soil textures are shown in grey color. The PFSC stabilized contaminated soil specimens with DOC ranging from 75% and 85% have visible pores and soil particle boundaries. The soil particles pressed against each other and the particle boundaries disappeared when the DOC were higher than 90%. The reduction of porosity resulted in the increasing of UCS and the decreasing of k_{w} (Fig. 1(a) and Fig. 1(b)) (Xue et al., 2014). Furthermore, the porosity affects the availability of O_2 (van Verseveld and Gebert, 2020), therefore the decrease in porosity resulted in a decreasing in the Eh (Fig. 1(d)). The pore space geometry is determined by soil texture and DOC (van Verseveld and Gebert, 2020). The porosities of PFSC stabilized contaminated soil specimens decreased with the increasing of DOC which resulted in the decrease of As and Sb D^{obs} (Table S4, Table 1, and Table S5-S10).

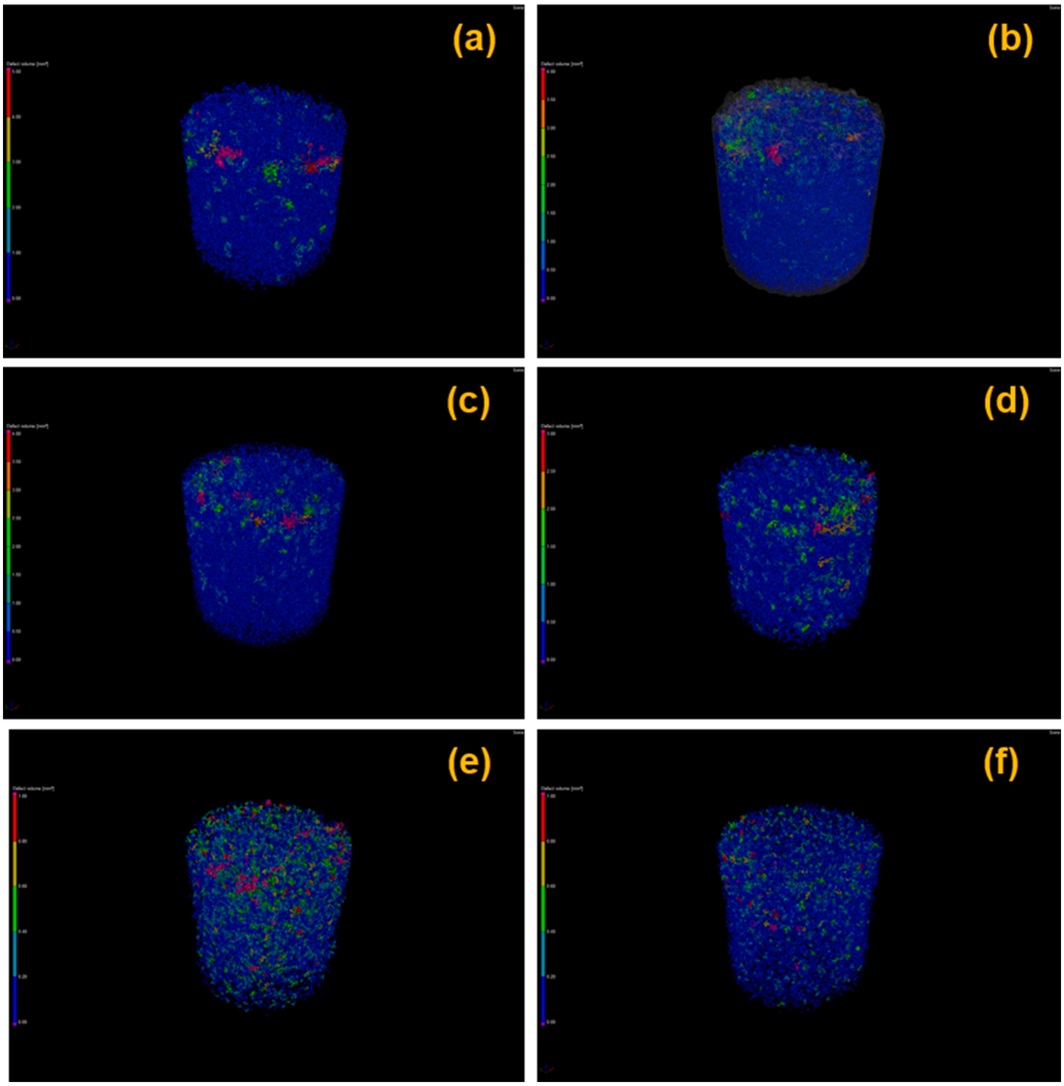

Fig. 3. CT analysis results of PFSC stabilized contaminated soil specimens compacted with degrees of (a) 75%, (b) 80%, (c) 85%, (d) 90%, (e) 93%, and (f) 96%.

3.5. XPS analysis

The survey spectra of PFSC stabilized contaminated soil samples compacted with different degrees are shown in Fig. S5, which revealed As, Sb, and Fe were the common elements in soils. Details in As 2p, Sb 3d, and Fe 2p orbits for PFSC stabilized contaminated soils with DOC of 75%, 90%, and 96% are shown in Fig. 4. For the survey of As 2p, the photoelectron peak at 1326.5 eV corresponded to the binding energy (B.E.) of As(V), while 1327.4 eV corresponded to the B.E. of As(III). Similarly, the photoelectron peak at 531.9 eV corresponded to the B.E. of Sb (V), while 532.7 eV corresponded to the B.E. of Sb(III). Furthermore, the photoelectron peaks at 712.5, 714.3, and 725.2 eV corresponded to the B.E. of Fe(III), while 710.0 and 711.3 eV corresponded to the B.E. of Fe (II), respectively. XPS results suggested that DOC affected the element species on PFSC stabilized contaminated soils.

Percentages of As(V) and As(III), Sb(V) and Sb(III), and Fe(III) and Fe (II) to total As, Sb, and Fe were calculated, respectively, and the results were marked on Fig. 4 and summarized in Table S11. The high-resolution spectrum of As 2p, Sb 3d, and Fe 2p indicated that As, Sb, and Fe predominantly existed in As(V), Sb(V), and Fe(III) (75.6%, 84.5%, and 74.4% atomic ratios for As(V), Sb(V), and Fe(III), respectively) forms for compaction degree of 75% according to peak areas. As the DOC of soil specimen increased, the percentages of As(V), Sb(V), and Fe(III) decreased from 75.6% to 47.2%, 84.5% to 71.6%, and 74.3% to 64.4% while the percentages of As(III), Sb(III), and Fe(II) increased from 24.4% to 52.8%, 15.5% to 28.4%, and 25.7% to 35.6%, respectively. The DOC affects the element species through influencing the availability the O_2 and then influencing the Eh of PFSC stabilized contaminated soils (van Verseveld and Gebert, 2020). The interactive effects of pE and pH on As and Sb species can be illustrated using pE-pH diagrams (Fig. 5). In which, pE = Eh/0.059 V at 25℃ and Eh is the equilibrium redox potential relative to the oxidation of H_2(g). As (V) and Sb(V) are the predominant As and Sb forms. As(V) and Sb(V) were partial reduced to As (III) and Sb(III) with increasing DOC. The toxicities and mobilities of As

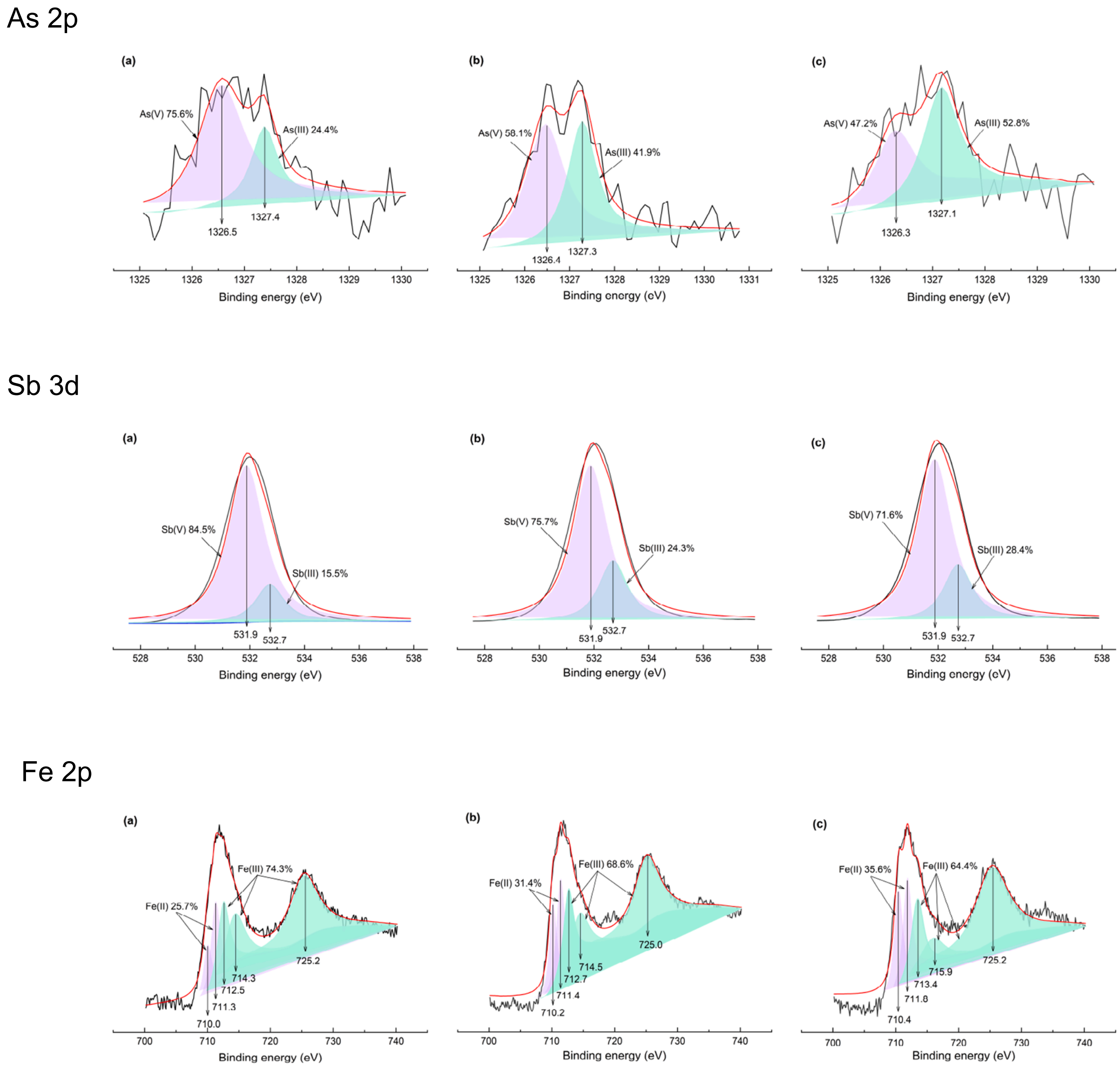

Fig. 4. XPS spectra of As 2p, Sb 3d, and Fe 2p for PFSC stabilized contaminated soil samples compacted with degrees of (a) 75%, (b) 90%, and (c) 96%.

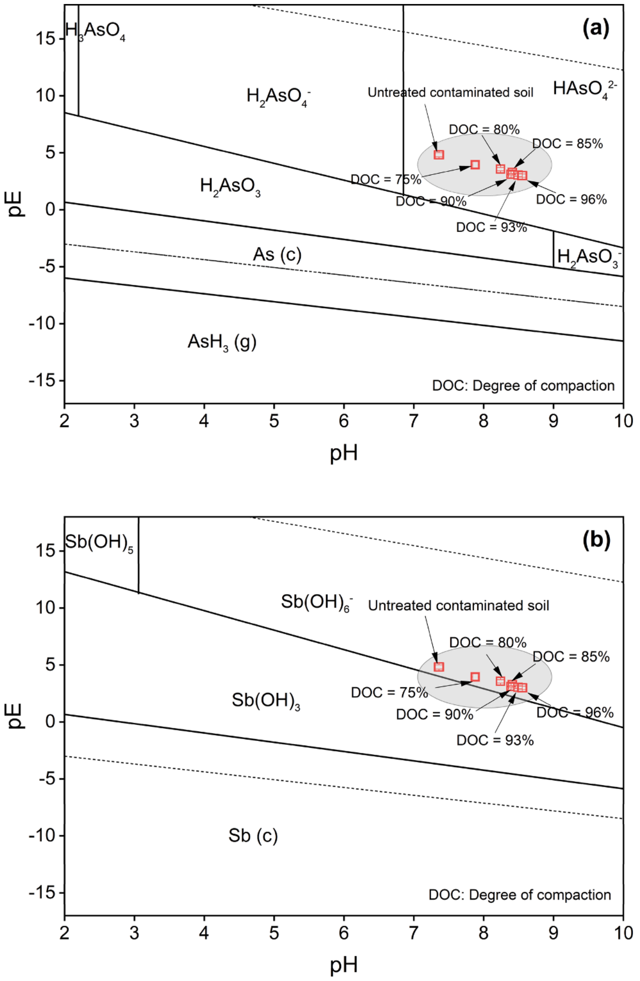

Fig. 5. The pE-pH diagram for (a) As and (b) Sb. Red rectangles indicate the pE and pH values of PFSC stabilized contaminated soil samples compacted with different degrees. (c) = crystalline, (g) = gas. Dashed lines indicate environmental redox limits imposed by the dissociation of water to H_2 (g) and O_2 (g).

and Sb are dependent on their species as well as the species of Fe (Wilson et al., 2010). The reduction of Fe(III) drives chemical reactions that iron minerals on which As and Sb are bound and contribute to the releases of As and Sb (Michael, 2013). The transformations of As and Sb from As(V) to As(III) and from Sb(V) to Sb(III) as the DOC increase were adverse for their toxicities and mobilities reduction. However, the effectiveness of using PFSC for As and Sb contaminated soil stabilization and the long-term environmental safety of stabilized contaminated soil result from the comprehensive effect of chemical specie transformation and pore filling. The variations of metalloids leached concentrations and D^{obs} with the DOC suggested the influence of pore filling was more significant than specie transformation.

4. Discussion

4.1. Comparison of batch and semi-dynamic leaching concentrations

Batch leaching test and semi-dynamic leaching test are standard leaching protocols available for evaluating the efficiency of PFSC stabilization and the mobilities of As and Sb in PFSC stabilized contaminated soils. The batch leaching test is the mostly commonly employed as a performance indicator and a remedial target of contaminated soil stabilization (Feng et al., 2021; Xia et al., 2019b; Zhou et al., 2022a). However, the batch leaching test is criticized for not reflecting the actual field conditions and contaminants leaching may be overestimated because of the necessitate size reduction of soil, and it is less accurate for evaluating the release from monolithic. Semi-dynamic test is designed specifically considering the low permeability and monolithic characteristic of contaminated soil after treatment, which can simulate in a more realistic leaching conditions of contaminants (Li et al., 2017b). Fig. 6 shows the As and Sb leached fractions obtained from batch and semi-dynamic leaching tests for PFSC stabilized contaminated soil specimens compacted with different degrees. Metalloids leached fractions obtained from semi-dynamic leaching test were higher than that of batch leaching test. This may be attributed to the higher solid/liquid ratio and the longer leaching time under semi-dynamic leaching test resulted in the higher amounts of metalloids for release. The agglutination of contaminated soil particle caused by PFSC stabilization was weaker than that of cementitious materials, such as Portland cement, ground granulated blast furnace slag-magnesium oxide (GGBS-MgO). When the contaminated soil treated by cementitious materials, the hydrated products formed in the soil matrix would fill the pore space and block the metalloids leaching flow paths. However, the exposure pathway of metalloids was not dramatically reduced in PFSC stabilized contaminated soil specimen. These resulted in the D^{obs} of metalloids released from PFSC stabilized contaminated were orders of magnitude higher than that of cementitious materials treated soils. (Li et al., 2017b) summarized the D^{obs} of As released from cement solidified soils, which ranged from 7.07×10^{-20} to 1.44×10^{-17} m^2 s^{-1}, and much lower than that in this study, which varied in the range of 4.65×10^{-11} to 1.92×10^{-8} m^2 s^{-1} for PFSC stabilized contaminated soil specimens compacted with different degrees.

4.2. DOC influence mechanisms

The leachabilities of As and Sb in the soil strongly depend upon their valence states (Wilson et al., 2010). Both As and Sb have a strong affinity to Fe oxides and hydroxides, which also influence the metalloids' mobilities in the environment. DOC effects the stabilization efficiency by changing the soil pH and Eh values (Fig. 1(d)), which drive the valence state transformation (Fig. 4) and Fe minerals dissolution. In reducing environments with high DOC, anoxic conditions drives chemical reactions that dissolve iron minerals on which As and Sb are bound (Michael, 2013) and the chemical species transfer from As(V) to As(III) and from Sb(V) to Sb(III), respectively. Fig. 7 shows the relationship between As and Sb leached fractions and element valence states for PFSC stabilized contaminated soil specimens compacted with degrees of 75%, 90%, and 96%, respectively. DOC has a greater influence on As and Sb leached fractions obtained from semi-dynamic leaching test than that of

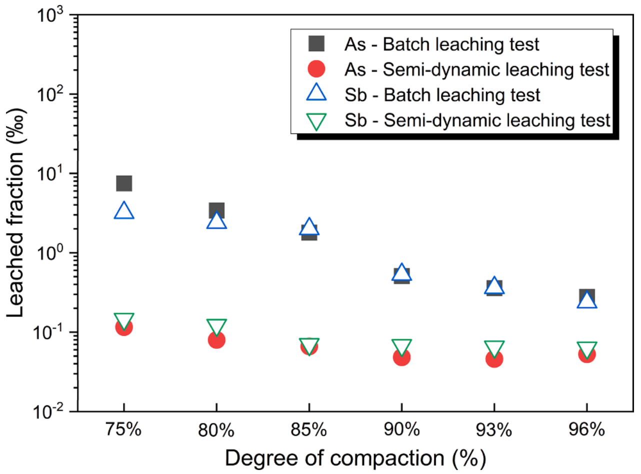

Fig. 6. As and Sb cumulative leached fractions obtained from batch and semi-dynamic leaching tests for PFSC stabilized contaminated soil specimens compacted with different degrees.

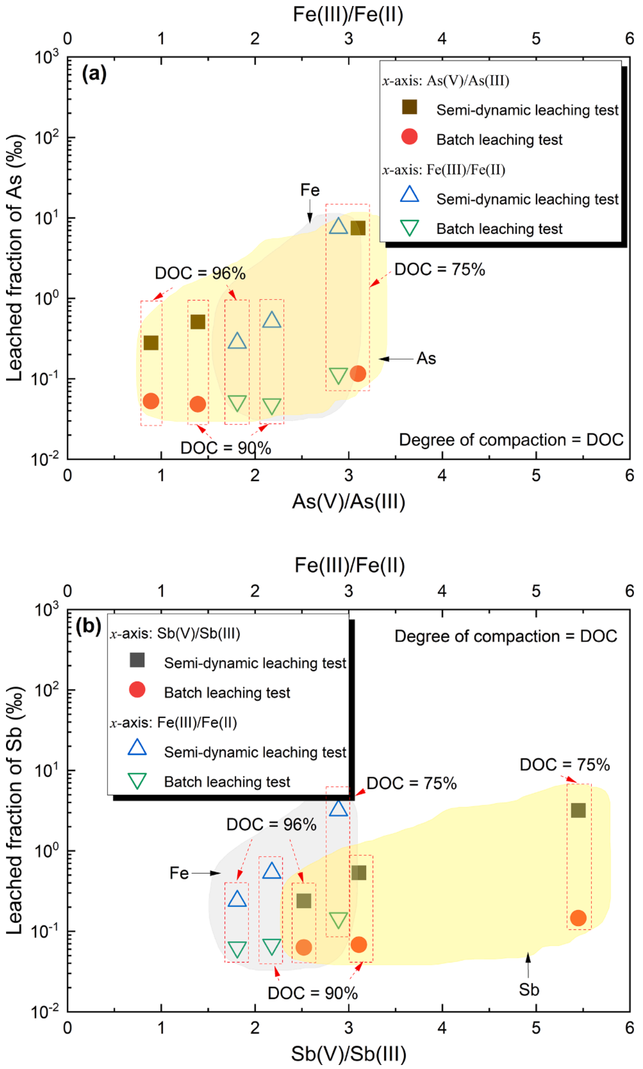

Fig. 7. Relationship between (a) As and (b) Sb cumulative leached fractions and element chemical species for PFSC stabilized contaminated soil specimens compacted with degrees of 75%, 90%, and 96%.

batch leaching test. Furthermore, As and Sb have wider valence states transformation areas than that of Fe suggest that As and Sb more easily influenced by DOC than Fe. The redox limits for As and Sb redox reactions (Wilson et al., 2010) indicate that As(V) and Sb(V) will both be reduced to trivalent state after Fe(III) is reduced to Fe(II). Only a small amount of Fe(III) was reduced to Fe(II) may attributed to a low percentage of Fe was existed in amorphous phases and goethite. More attention should be paid to metalloid release caused by Fe reduction with DOC increase in high Fe content contaminated soils.

4.3. DOC control in practice implication

Constituent leachability, UCS, and k_w were the three mostly important properties for the evaluation of stabilization practice. Leaching concentration was the most important of these, and it should always be given precedence because it determined if the practice was successful. The impact of DOC on UCS needed to be given more consideration when the stabilized contaminated was reused as civil engineering materials. Low permeability of stabilized contaminated soil was beneficial to reduce the migration of contaminants to the surrounding soil and groundwater. The UCS of soil specimen increased while the k_w of soil specimen decreased with increasing DOC. The As leached concentration decreased before the DOC reached 90%, and then an increased trend was observed with DOC further increased to 96%. Therefore, the DOC of nearly 90% was recommended in the practice implication of PFSC stabilization.

5. Conclusions

Various geoenvironmental property tests, including metalloids leached concentrations, unconfined compressive strength (UCS), and hydraulic conductivity (k_w) were performed on As and Sb co-contaminated soil stabilized by PFSC compacted with different degrees, and the influence mechanisms were analyzed. The main conclusions were as follows:

(1) The UCS of soil specimen increased with the increasing of DOC, while the k_w decreased as the DOC increased. The As leached concentrations decreased first and then increased slightly before and after the DOC of 90%, whereas the Sb leached concentrations decreased as the DOC increased. The DOC affects the availability of oxygen, resulting in a decrease in Eh as the DOC increases.
(2) As the DOC of soil specimen increased, the cumulative fractions of metalloids decreased. The releases of As and Sb from soil specimens were main controlled by diffusion. The mean D^{obs} of metalloids decreased with the increasing of DOC. Furthermore, the mean D^{obs} for metalloids released form soil specimen with a DOC of 96% were 3 and 2 orders of magnitude lower than that of 75%, respectively.
(3) CT analyze results indicated the macropore number and macropore size in soil specimens were reduced with the increasing DOC. Compaction increased the UCS and reduced the k_w of PFSC stabilized contaminated soil specimens by reducing their porosities. Compaction promoted the specie transformation of As, Sb, and Fe from As(V) to As(III), from Sb(V) to Sb(III), and Fe(III) to Fe(II). The pore filling and chemical specie transformation jointly determined the releases of As and Sb from PFSC stabilized contaminated soil specimens.

Declaration of Competing Interest

The authors declare that they have no known competing financial interests or personal relationships that could have appeared to influence the work reported in this paper.

Acknowledgments

This paper was written to support the National Key Research and Development Program of China (No. 2019YFC1806000), National Natural Science Foundation of China (Grant No. 41877248, No. 42177133), Postgraduate Research & Practice Innovation Program of Jiangsu Province (KYCX18-0124), and Nanjing Planned Projects for Postdoctoral Research Funds (No. 2021040).

Appendix A. Supplementary data

Supplementary data to this article can be found online at https://doi.org/10.1016/j.catena.2022.106634.

References

Ajith, N., Bhattacharyya, K., Ipte, P.R., Satpati, A.K., Tripathi, A.K., Verma, R., Swain, K. K., 2019. Interaction of arsenic(III) and arsenic(V) on manganese dioxide: XPS and electrochemical investigations. J. Environ. Sci. Health Part A 54, 277–285. https://doi.org/10.1080/10934529.2018.1544478.

Álvarez-Ayuso, E., Otones, V., Murciego, A., García-Sánchez, A., 2013. Evaluation of different amendments to stabilize antimony in mining polluted soils. Chemosphere 90, 2233–2239. https://doi.org/10.1016/j.chemosphere.2012.09.086.

An, J.S., Jeong, B.Y., Nam, K., 2019. Evaluation of the effectiveness of in situ stabilization in the field aged arsenic-contaminated soil: Chemical extractability and biological response. J. Hazard. Mater. 367, 137–143. https://doi.org/10.1016/j.jhazmat.2018.12.050.

Bagherifam, S., Lakzian, A., Fotovat, A., Khorasani, R., Komarneni, S., 2014. In situ stabilization of As and Sb with naturally occurring Mn, Al and Fe oxides in a calcareous soil: Bioaccessibility, bioavailability and speciation studies. J. Hazard. Mater. 273, 247–252. https://doi.org/10.1016/j.jhazmat.2014.03.054.

Fawcett, S.E., Jamieson, H.E., Nordstrom, D.K., McCleskey, R.B., 2015. Arsenic and antimony geochemistry of mine wastes, associated waters and sediments at the Giant Mine, Yellowknife, Northwest Territories, Canada. Appl. Geochem. 62, 3–17. https://doi.org/10.1016/j.apgeochem.2014.12.012.

Feng, Y.S., Du, Y.J., Xia, W.Y., Reddy, K.R., 2020. Pilot-scale field investigation of ex situ solidification/stabilization of soils with inorganic contaminants using two novel binders. Acta Geotech. 15, 1467–1480. https://doi.org/10.1007/s11440-019-00835-5.

Feng, Y.S., Du, Y.J., Zhou, A.N., Zhang, M., Li, J.S., Zhou, S.J., Xia, W.Y., 2021. Geoenvironmental properties of industrially contaminated site soil solidified/stabilized with a sustainable by-product-based binder. Sci. Total Environ. 765, 142778 https://doi.org/10.1016/j.scitotenv.2020.142778.

Feng, Y.S., Zhou, S.J., Zhou, A.N., Xia, W.Y., Li, J.S., Wang, S., Du, Y.J., 2022. Reuse of a contaminated soil stabilized by a low-carbon binder as roadway subgrade material and mechanical performance evaluation. Eng. Geol. 303, 106656 https://doi.org/10.1016/j.enggeo.2022.106656.

Filella, M., Belzile, N., Chen, Y.W., 2002. Antimony in the environment: A review focused on natural waters II. Relevant solution chemistry 21.

Fritzsche, A., Dienemann, H., Dudel, E.G., 2006. Arsenic fixation on iron-hydroxide-rich and plant litter-containing sediments in natural environments. Environ. Geol. 51, 133–142. https://doi.org/10.1007/s00254-006-0315-0.

Frost, R.R., Griffin, R.A., 1977. Effect of pH on adsorption of arsenic and selenium from landfill leachate by clay minerals. Soil Sci. Soc. Am. J. 41, 53–57. https://doi.org/10.2136/sssaj1977.03615995004100010019x.

Huang, L.H., Zhou, S.J., Jin, F., Huang, J., Bao, N., 2014. Characterization and mechanism analysis of activated carbon fiber felt-stabilized nanoscale zero-valent iron for the removal of Cr(VI) from aqueous solution. Colloids Surf., A 447, 59–66. https://doi.org/10.1016/j.colsurfa.2014.01.037.

Johnston, S.G., Bennett, W.W., Doriean, N., Hockmann, K., Karimian, N., Burton, E.D., 2020. Antimony and arsenic speciation, redox-cycling and contrasting mobility in a mining-impacted river system. Sci. Total Environ. 710, 136354 https://doi.org/10.1016/j.scitotenv.2019.136354.

Ketcham, R.A., 2005. Three-dimensional grain fabric measurements using high-resolution X-ray computed tomography. J. Struct. Geol. 27, 1217–1228. https://doi.org/10.1016/j.jsg.2005.02.006.

Ko, M.S., Kim, J.Y., Bang, S., Lee, J.S., Ko, J.I., Kim, K.W., 2012. Stabilization of the As-contaminated soil from the metal mining areas in Korea. Environ. Geochem. Health 34, 143–149. https://doi.org/10.1007/s10653-011-9407-1.

Ko, M.S., Park, H.S., Lee, J.U., 2017. Influence of indigenous bacteria stimulation on arsenic immobilization in field study. Catena 148, 46–51. https://doi.org/10.1016/j.catena.2016.08.022.

Krysiak, A., Karczewska, A., 2007. Arsenic extractability in soils in the areas of former arsenic mining and smelting, SW Poland. Sci. Total Environ. 379, 190–200. https://doi.org/10.1016/j.scitotenv.2006.09.031.

Leuz, A.K., Mönch, H., Johnson, C.A., 2006. Sorption of Sb(III) and Sb(V) to goethite: Influence on Sb(III) oxidation and mobilization. Environ. Sci. Technol. 40, 7277–7282. https://doi.org/10.1021/es061284b.

Li, J.P., Ding, Y., Wang, K.L., Li, N., Qian, G.R., Xu, Y.F., Zhang, J., 2020. Comparison of humic and fulvic acid on remediation of arsenic contaminated soil by electrokinetic technology. Chemosphere 241, 125038. https://doi.org/10.1016/j.chemosphere.2019.125038.

Li, J.S., Beiyuan, J., Tsang, D.C.W., Wang, L., Poon, C.S., Li, X.D., Fendorf, S., 2017a. Arsenic-containing soil from geogenic source in Hong Kong: Leaching characteristics and stabilization/solidification. Chemosphere 182, 31–39. https://doi.org/10.1016/j.chemosphere.2017.05.019.

Li, J.S., Wang, L., Tsang, D.C.W., Beiyuan, J., Poon, C.S., 2017b. Dynamic leaching behavior of geogenic As in soils after cement-based stabilization/solidification. Environ. Sci. Pollut. Res. 24, 27822–27832. https://doi.org/10.1007/s11356-017-0266-x.

Liu, C.P., Luo, C.L., Gao, Y., Li, F.B., Lin, L.W., Wu, C.A., Li, X.D., 2010. Arsenic contamination and potential health risk implications at an abandoned tungsten mine, southern China. Environ. Pollut. 158, 820–826. https://doi.org/10.1016/j.envpol.2009.09.029.

Madejón, P., Domínguez, M.T., Gil-Martínez, M., Navarro-Fernández, C.M., Montiel-Rozas, M.M., Madejón, E., Murillo, J.M., Cabrera, F., Marañón, T., 2018. Evaluation of amendment addition and tree planting as measures to remediate contaminated soils: The Guadiamar case study (SW Spain). Catena 166, 34–43. https://doi.org/10.1016/j.catena.2018.03.016.

Martínez, I., Chervet, A., Weisskopf, P., Sturny, W.G., Rek, J., Keller, T., 2016. Two decades of no-till in the Oberacker long-term field experiment: Part II. Soil porosity and gas transport parameters. Soil Tillage Res. 163, 130–140. https://doi.org/10.1016/j.still.2016.05.020.

Michael, H.A., 2013. An arsenic forecast for China. Science 341, 852–853. https://doi.org/10.1126/science.1242212.

Nakamaru, Y., Tagami, K., Uchida, S., 2006. Antimony mobility in Japanese agricultural soils and the factors affecting antimony sorption behavior. Environ. Pollut. 141, 321–326. https://doi.org/10.1016/j.envpol.2005.08.040.

Ona-Nguema, G., Morin, G., Juillot, F., Calas, G., Brown, G.E., 2005. EXAFS Analysis of arsenite adsorption onto two-line ferrihydrite, hematite, goethite, and lepidocrocite. Environ. Sci. Technol. 39, 9147–9155. https://doi.org/10.1021/es050889p.

Quiroz, W., Astudillo, F., Bravo, M., Cereceda-Balic, F., Vidal, V., Palomo-Marín, M.R., Rueda-Holgado, F., Pinilla-Gil, E., 2016. Antimony speciation in soils, sediments and volcanic ashes by microwave extraction and HPLC-HG-AFS detection. Microchem. J. 129, 111–116. https://doi.org/10.1016/j.microc.2016.06.016.

Shetty, R., Vidya, C.S.N., Vaculík, M., 2021. Comparison of the single and combined effects of arsenic and antimony on growth and physiology of giant reed (Arundo donax L.). Environ. Sci. Pollut. Res. 28, 55476–55485. https://doi.org/10.1007/s11356-021-14870-x.

Smith, E., Naidu, R., Alston, A.M., 1999. Chemistry of Arsenic in Soils: I. Sorption of arsenate and arsenite by four Australian soils. J. Environ. Quality 28, 1719–1726. https://doi.org/10.2134/jeq1999.00472425002800060005x.

Telford, K., Maher, W., Krikowa, F., Foster, S., Ellwood, M.J., Ashley, P.M., Lockwood, P.V., Wilson, S.C., 2009. Bioaccumulation of antimony and arsenic in a highly contaminated stream adjacent to the Hillgrove Mine, NSW, Australia. Environ. Chem. 6, 133. https://doi.org/10.1071/EN08097.

Van Verseveld, C.J.W., Gebert, J., 2020. Effect of compaction and soil moisture on the effective permeability of sands for use in methane oxidation systems. Waste Manage. 107, 44–53. https://doi.org/10.1016/j.wasman.2020.03.038.

Vrînceanu, N.O., Motelică, D.M., Dumitru, M., Calciu, I., Tănase, V., Preda, M., 2019. Assessment of using bentonite, dolomite, natural zeolite and manure for the immobilization of heavy metals in a contaminated soil: The Copșa Mică case study (Romania). Catena 176, 336–342. https://doi.org/10.1016/j.catena.2019.01.015.

Wang, F., Wang, H.L., Al-Tabbaa, A., 2015a. Time-dependent performance of soil mix technology stabilized/solidified contaminated site soils. J. Hazard. Mater. 286, 503–508. https://doi.org/10.1016/j.jhazmat.2015.01.007.

Wang, F., Wang, H.L., Jin, F., Al-Tabbaa, A., 2015b. The performance of blended conventional and novel binders in the in-situ stabilisation/solidification of a contaminated site soil. J. Hazard. Mater. 285, 46–52. https://doi.org/10.1016/j.jhazmat.2014.11.002.

Wang, Y., Li, X., Zhang, B., Wu, Y.F., 2014. Meso-damage cracking characteristics analysis for rock and soil aggregate with CT test. Sci. China Technol. Sci. 57, 1361–1371. https://doi.org/10.1007/s11431-014-5578-1.

Wilson, S.C., Lockwood, P.V., Ashley, P.M., Tighe, M., 2010. The chemistry and behaviour of antimony in the soil environment with comparisons to arsenic: A critical review. Environ. Pollut. 158, 1169–1181. https://doi.org/10.1016/j.envpol.2009.10.045.

Xia, W.Y., Du, Y.J., Li, F.S., Guo, G.L., Yan, X.L., Li, C.P., Arulrajah, A., Wang, F., Wang, S., 2019a. Field evaluation of a new hydroxyapatite based binder for *ex-situ* solidification/stabilization of a heavy metal contaminated site soil around a Pb-Zn smelter. Constr. Build. Mater. 210, 278–288. https://doi.org/10.1016/j.conbuildmat.2019.03.195.

Xia, W.Y., Du, Y.J., Li, F.S., Li, C.P., Yan, X.L., Arulrajah, A., Wang, F., Song, D.J., 2019b. In-situ solidification/stabilization of heavy metals contaminated site soil using a dry jet mixing method and new hydroxyapatite based binder. J. Hazard. Mater. 369, 353–361. https://doi.org/10.1016/j.jhazmat.2019.02.031.

Xu, D.M., Fu, R.B., Wang, J.X., Shi, Y.X., Guo, X.P., 2021. Chemical stabilization remediation for heavy metals in contaminated soils on the latest decade: Available stabilizing materials and associated evaluation methods–A critical review. J. Cleaner Prod. 321, 128730 https://doi.org/10.1016/j.jclepro.2021.128730.

Xue, Q., Li, J.S., Liu, L., 2014. Effect of compaction degree on solidification characteristics of Pb-contaminated soil treated by cement: Effect of compaction degree on solidification characteristics. Clean: Soil, Air, Water 42, 1126–1132. https://doi.org/10.1002/clen.201300345.

Yuan, C., Chiang, T.S., 2008. Enhancement of electrokinetic remediation of arsenic spiked soil by chemical reagents. J. Hazard. Mater. 152, 309–315. https://doi.org/10.1016/j.jhazmat.2007.06.099.

Zhang, G.P., Liu, C.Q., Liu, H., Hu, J., Han, G.L., Li, L., 2009. Mobilisation and transport of arsenic and antimony in the adjacent environment of Yata gold mine, Guizhou province, China. J. Environ. Monit. 11, 1570. https://doi.org/10.1039/b908612a.

Zhang, T., Yang, Y.L., Liu, S.Y., 2020. Application of biomass by-product lignin stabilized soils as sustainable Geomaterials: A review. Sci. Total Environ. 728, 138830 https://doi.org/10.1016/j.scitotenv.2020.138830.

Zhao, L., Ding, Z.L., Sima, J.K., Xu, X.Y., Cao, X.D., 2017. Development of phosphate rock integrated with iron amendment for simultaneous immobilization of Zn and Cr(VI) in an electroplating contaminated soil. Chemosphere 182, 15–21. https://doi.org/10.1016/j.chemosphere.2017.05.004.

Zhou, S.J., Du, Y.J., Feng, Y.S., Sun, H.Y., Xia, W.Y., Yuan, H., 2022a. Stabilization of arsenic and antimony co-contaminated soil with an iron-based stabilizer: Assessment of strength, leaching and hydraulic properties and immobilization mechanisms. Chemosphere 301, 134644. https://doi.org/10.1016/j.chemosphere.2022.134644.

Zhou, S.J., Du, Y.J., Sun, H.Y., Yuan, H., Feng, Y.S., Xia, W.Y., 2022b. Evaluation of the effectiveness of *ex-situ* stabilization for arsenic and antimony contaminated soil: Short-term and long-term leaching characteristics. Sci. Total Environ. 848, 157646 https://doi.org/10.1016/j.scitotenv.2022.157646.